Chapter 3. Objectives

This chapter summarizes the motivations and objectives of this study. It is also a guide to the subsequent chapters and an overview of the contributions made in this work.

3.1 Objectives

The overriding objective of this study is to advance the understanding of trickle flow hydrodynamics, with specific emphasis on the phenomenon of hydrodynamic multiplicity. This can be broken down into three objectives:

Objective 1. The establishment of a **conceptual framework** by which the phenomena alluded to in the previous chapter can be studied experimentally. The limiting cases of hydrodynamic multiplicity introduced in Table 5 are proposed as such a framework.

Objective 2. Closely coupled with this, is the objective of attaining further **experimental insight** into the role of bed and system conditions and their (possible) influence(s) on the extent of hydrodynamic multiplicity. This involves clarification of the relationship between the bed structure and flow multiplicity. Central to this issue are the questions of the temporal stability, spatial liquid distribution and reproducibility of the flow pattern, as well as the roles of surface tension and particle characteristics. Here, the idea is not to investigate all possible permutations of operating variables but rather to extract the fundamental trends (in accordance with the strategy in Figure 1).

Objective 3. The identification of the probable **mechanism responsible for hydrodynamic multiplicity**. An improved understanding of this mechanism should account for both manifestations of multiplicity: hysteresis loops and pre-wetting modes, and an outline of how the mechanism is to be incorporated in existing hydrodynamic models should be clear.

A further illustration of the impact of hydrodynamic multiplicity on trickle bed reactor performance is given in Chapter 8. First, experimental verification of pressure drop hysteresis in an industrial reactor is reported. Second, an experimental reaction case study (α-methyl styrene hydrogenation) is presented that illustrates the impact of multiplicity on conversion.

3.2 Thesis Structure

The objectives outlined above are addressed in subsequent chapters as outlined in Table 10. Together with Figure 1, this table is both a guide to the thesis and a list of the major contributions of this work.

Table 10. Thesis structure

Section	Issues Addressed
Chapter 2	Re-interprets literature in terms of proposed framework (section 2.2.2) and identifies multiplicity trends
Chapter 4	Experimental investigations into bed-scale hydrodynamics, identifying further multiplicity trends
Chapter 5	Preliminary experimental investigation into cluster-of-particles scale hydrodynamics using established radiographic and tomographic techniques (further multiplicity trends identified)
Chapter 6	Advances the image processing strategy of the tomographic data in order to yield high definition volume images that are again used to identify the nature (and trends) of hydrodynamic multiplicity.
Chapter 7	Interpretation of all experimental results and multiplicity modelling at the pore scale
Chapter 8	Experimental verification of pressure drop multiplicity in an industrial reactor. Impact of hysteresis on reactor performance, proving the concept that multiplicity can be used to enhance reactor performance

Chapter 4. Bed-Scale Phenomena

This chapter addresses hydrodynamic multiplicity at the bed-scale through measurements of bed-averaged hydrodynamic parameters. This forms part 1 of the Additional Experimental Insights block in Figure 1 and partially satisfies Objective 2 (achieving further experimental insight into hydrodynamic multiplicity - as outlined in Chapter 3). This chapter starts with the experimental details and then presents the results in three sections: those obtained in beds of non-porous particles, those obtained in beds of porous particles and the effect of increased operating pressure on hydrodynamic multiplicity. In accordance with the strategy in Figure 1, the list of characteristic multiplicity trends are confirmed and extended by the work in this chapter. The updated list is given at the end of the chapter.

4.1 Experimental

The perennial problem of investigating trickle flow hydrodynamics is the inherent complexity. In this work, like all others, the amount of experimental data is limited to what is practically possible. The emphasis here is placed on augmenting the literature data where Chapter 2 and the conceptual framework have identified the need to do so. The focus is on uncovering the mechanism of hydrodynamic multiplicity through identifying the characteristic trends.

The experimental setup that was used to generate the bulk of the data in this chapter is shown in Figure 11 and experimental details are given in Table 11.

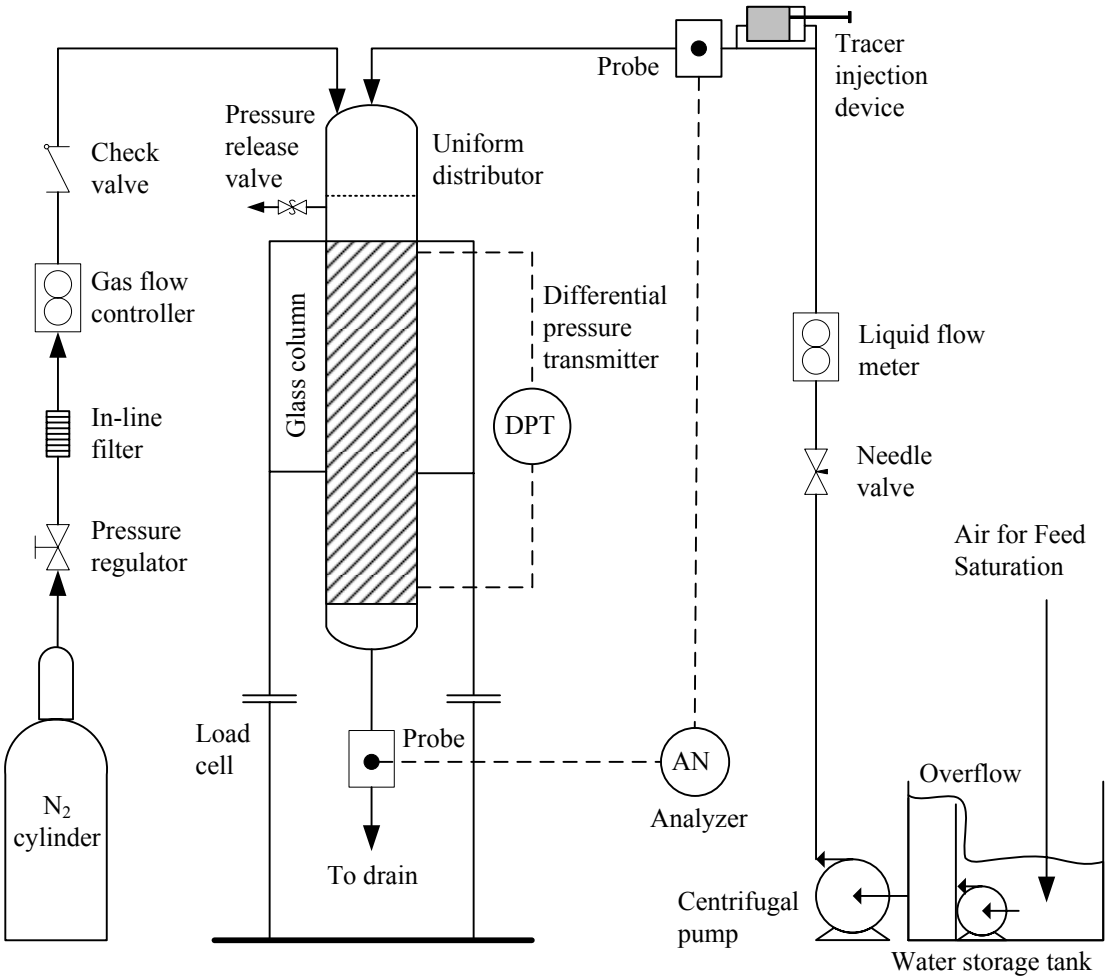

Figure 11. Experimental setup for bed scale experiments.

4.2 Multiplicity in Beds of Non-Porous Particles[1]

Table 7 shows that there has been no investigation into all five multiplicity modes for a single bed. It is imperative to confirm that the trends reported in literature are indeed due to flow peculiarities and not because of differences in the individual bed structures and experimental conditions.

[1] Data from this section was published in Chemical Engineering Science, Vol. 61, pg 7551-7562, 2006.

Table 11. Experimental details

Liquids	Water Water + Ethanol (20 %)
Gas	Nitrogen (87 kPa)
Surface tension	0.02-0.03 N/m, 0.07 N/m
Particles	3 mm non-porous glass spheres 3 × 3 mm porous extrudate 2.5 mm porous alumina spheres
Column diameter	68 mm
Bed length	850 mm
Liquid velocity	1.0 – 9.0 mm/s
Gas velocity	2.0 – 9.0 cm/s
Load cell	Revere Transducers Europe (accuracy: ±4 g)
Differential pressure transducer	Rosemount 3051CD (accuracy: ±10 Pa)
Dissolved oxygen probes	Rosemount 499ADO (resolution: 0.1 ppm)
Conductivity probes	Eutech PC5500 (accuracy: 0.1%)
Distributor drip point density	16000 points per m^2

For this reason, a set of experimental data was produced for the most common system in literature: 3 mm glass spheres, with water and low pressure nitrogen as fluids. Each multiplicity mode was established according to the framework introduced in Table 5. In addition to the pressure drop, the liquid holdup and the volumetric gas-liquid mass transfer coefficient were measured by the gravimetric method and the physical desorption of dissolved oxygen respectively over a range of gas and liquid velocities. All reported values are at steady state (no change in any of the hydrodynamics was observed after about 5 minutes at each operating condition). Additional experimental concerns are dealt with in detail in Loudon et al. (2006); here the emphasis is on interpreting the results. Figure 12 to Figure 14 show the pressure drop, holdup and mass transfer results as functions of liquid velocities. Figure 15 shows these parameters as functions of gas velocity at the highest liquid velocity (the highest liquid velocity is chosen because it was

not possible to achieve gas flow rate induced pulsing at lower liquid velocities). Note that each point represents the average of three experiments. Error bars are not shown since they coincide with the symbols themselves. Instead, the reproducibility for each parameter for each mode is reported in Table 12. The total average relative standard deviation is 4%, and this is considerably lower than the differences between the modes.

Table 12. Reproducibility of results

Parameter	**Average relative standard deviation (%)**					
	NPW	Levec	Super	Kan-Liquid	Kan-Gas	All modes
$\Delta P/\Delta z$	4.1	2.5	5.0	3.9	10.5	5.2
ε_L	2.9	1.5	1.7	1.5	0.6	1.6
$k_{GL}a_{GL}$	14.1	3.3	6.6	3.5	2.1	5.9

Several important conclusions can be made from this data. In Figure 12 there are two very clear regions, the upper branch consisting of the Kan-Liquid and Super modes and the lower branch consisting of the Non-pre-wetted and Levec modes. It is for this reason that several investigators (for example Jiang et al., 2000) only distinguish between “non-pre-wetted” and “pre-wetted” conditions. Figure 13 and Figure 14 however dispels this framework. In fact, Figure 15 shows that there are indeed five distinct multiplicity modes. In general, the present data confirm the trends that were extracted from literature in Chapter 2. Note that the data represents the average of three re-packings and that the reproducibility was good. This means that some general conclusions can be drawn about the hydrodynamic behaviour in each multiplicity mode and that all the different modes can be compared directly for the first time (since previous investigators did not investigate all the modes for the same system). A list of these conclusions follow.

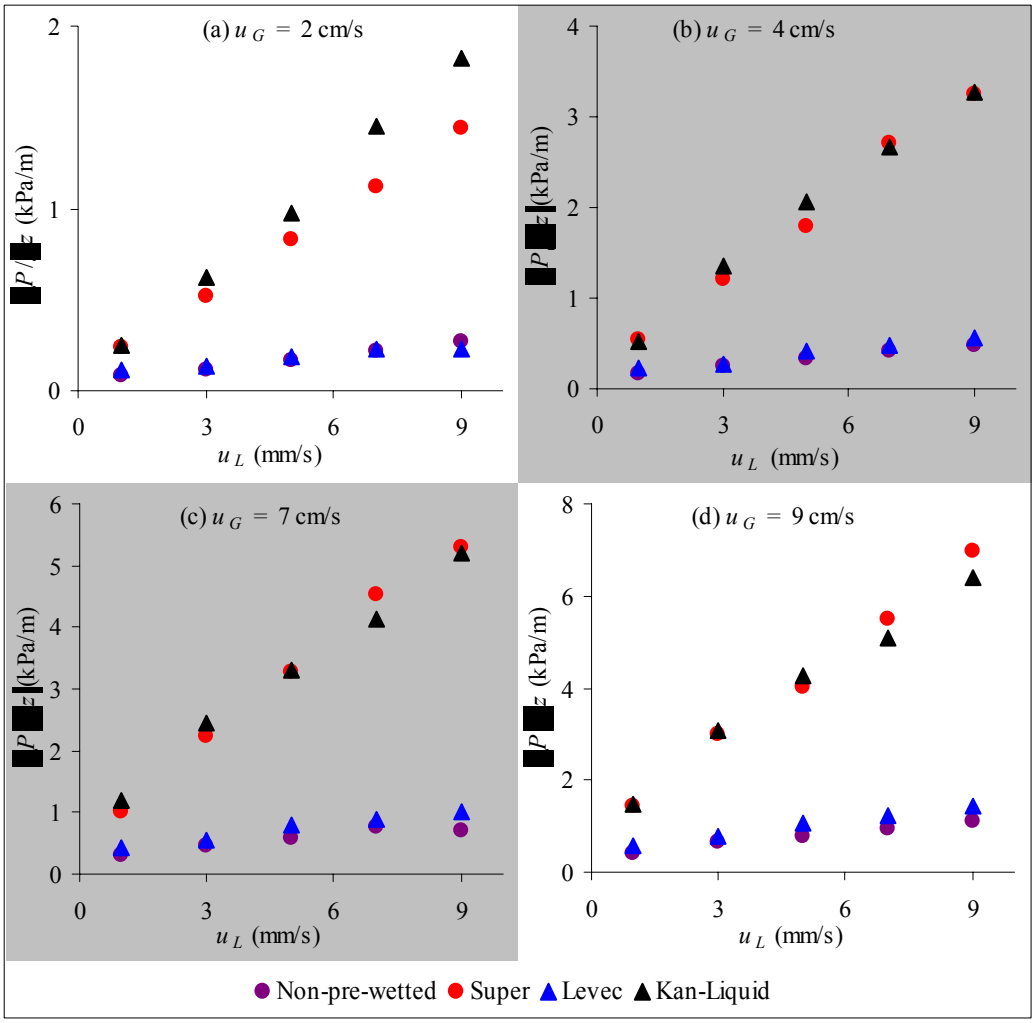

Figure 12. Pressure drop as a function of gas and liquid velocity

- The absolute upper limit of *pressure drop* is achieved in the Kan-Liquid/Super modes and the absolute lower limit is the Levec and Non-pre-wetted modes. The absolute upper limit for *holdup* is the Kan-Gas mode and the absolute lower limit is the Non-pre-wetted mode. The Levec mode is the lower limit for holdup that can be achieved in a pre-wetted bed, while the Super mode represents the upper limit for holdup and pressure drop where no flow rate above the operating rates were used. All five cases are therefore significant.

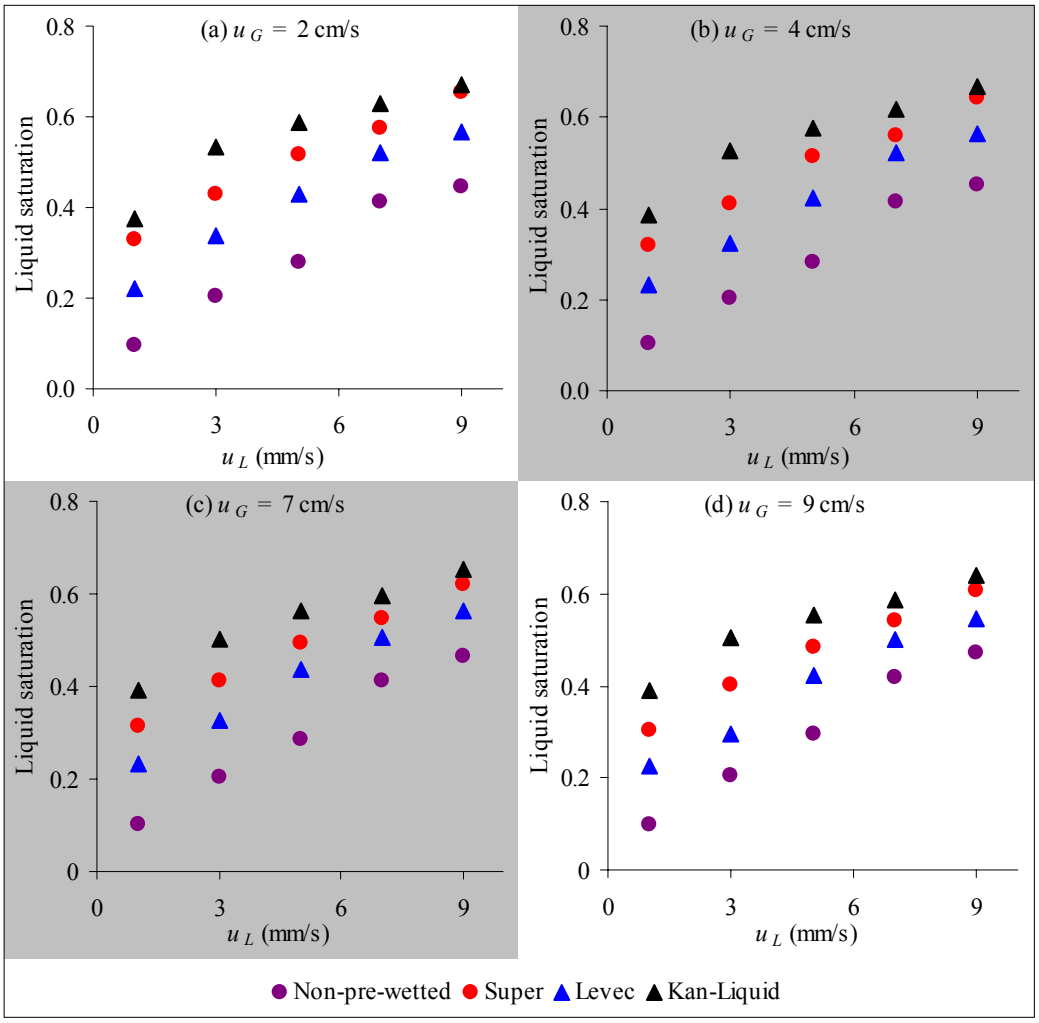

Figure 13. Liquid saturation ($\varepsilon_L/\varepsilon$) as a function of gas and liquid velocity

- The pressure drop in the upper limiting mode is between 2 and 8 times higher than that in the lower limiting mode. The holdup in the upper limiting case (Kan-Gas) can be up to 8 times higher than in the lower limiting case (Non-pre-wetted) and up to 4 times higher than the lower limiting case for pre-wetted beds (Levec mode). The gas-liquid mass transfer coefficient is up to 6 times higher in the upper limiting case (Super mode) than in the lower limiting case (Non-pre-wetted) and up to 2.4 times higher than the lower limiting case for pre-wetted beds (Levec mode). This emphasizes not only the importance of pre-wetting, but also the importance of the exact operating procedure and the flow history.

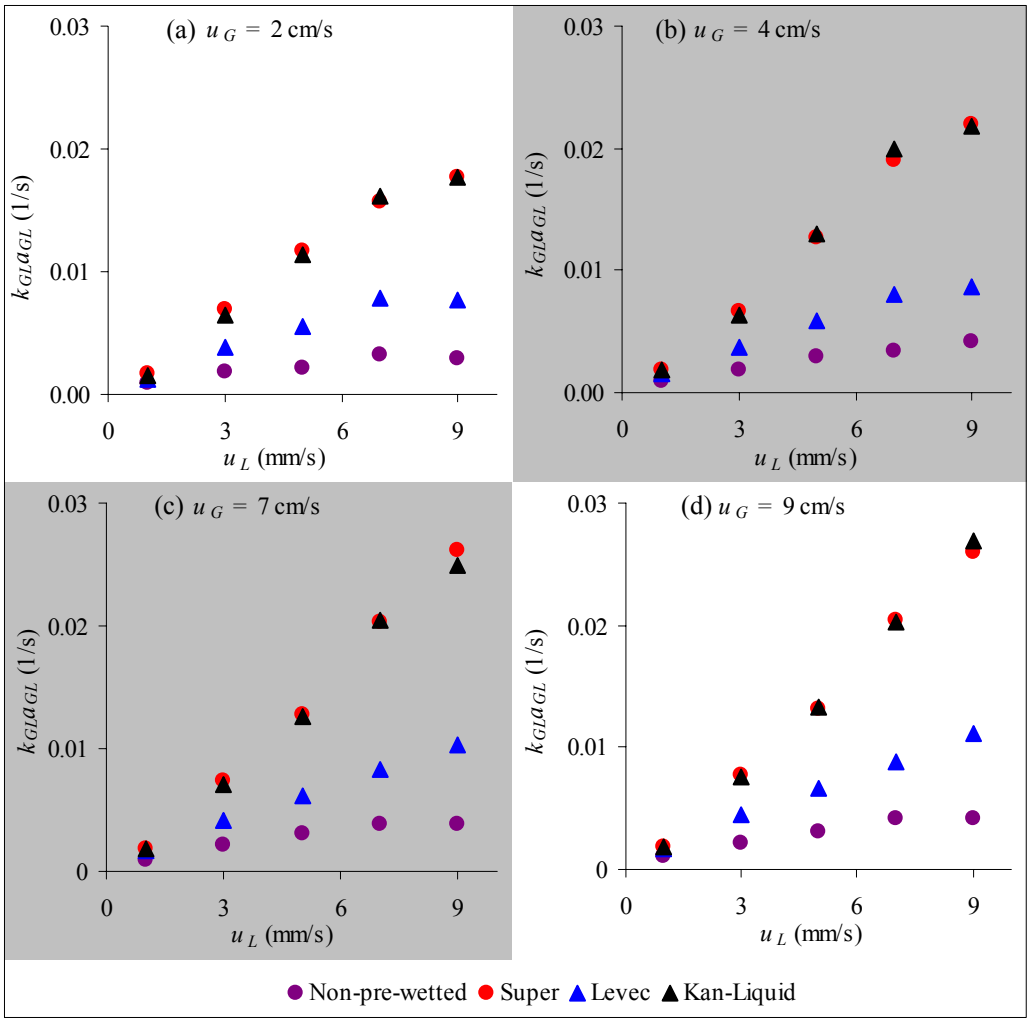

Figure 14. Volumetric gas-liquid mass transfer coefficient as a function of gas and liquid velocity

- In all the modes pressure drop, liquid holdup and gas-liquid mass transfer always increase with an increase in liquid velocity as expected from the increased liquid-solid drag that result in higher holdup. Pressure drop and gas-liquid mass transfer also increases with gas velocity and liquid holdup decreases with gas velocity in the Kan-Liquid, Kan-Gas, Super and Levec modes (as expected from the increased gas-liquid drag), but liquid holdup increases in the Non-pre-wetted mode as u_G increases. This is indicative of a second effect, namely that the increased gas-liquid drag serves to spread the liquid over the packing (and

therefore results in higher liquid-solid drag). Here, we see again the importance of liquid distribution in determining the hydrodynamics of the system.

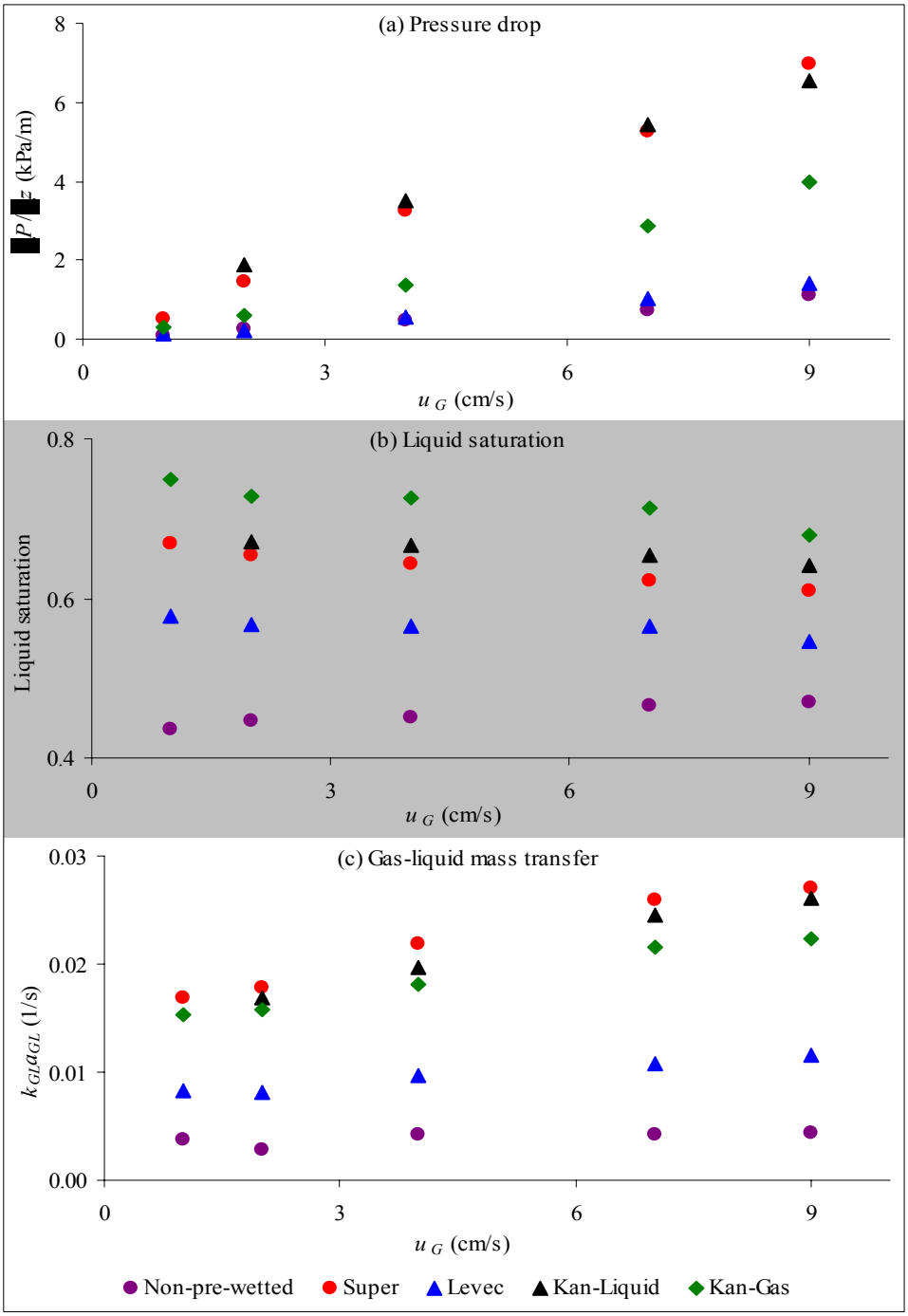

Figure 15. Pressure drop, liquid saturation and volumetric gas-liquid mass transfer coefficient as a function of gas velocity at u_L = 9 mm/s.

- The gas-liquid mass transfer coefficient is an indication of the "spreadedness" of the liquid. A uniform film that covers all the particles will have a much larger gas-liquid interfacial area than a rivulet that encompasses clusters of particles. This supports the idea of rivulet and film flow introduced by Christensen et al. (1986).
- The Non-pre-wetted and Levec modes show interesting behaviour in that their pressure drops are equal, but both holdup and gas-liquid mass transfer differ significantly. This means that pressure drop is a poor choice for distinguishing these modes. From Figure 12, Figure 14 and Figure 15 it appears that the Super and Kan-Liquid modes are very similar. This is a significant result because these modes are obtained through vastly different procedures (flooding vs. pulsing).
- An important result that will re-surface in Chapter 8 is the fact that the Kan-Liquid mode has a significantly higher $k_{GL}a_{GL}$ value than the Levec mode.
- The Kan-Gas mode presents a peculiarity: it has a higher holdup than any other mode (Figure 15b) but not the highest pressure drop (Figure 15a). This is very much against the conventional understanding (that is based mostly on the other modes).

The observations listed above are the essential features that a hydrodynamic multiplicity model should incorporate and form part of the list of multiplicity trends.

It is also informative to evaluate present data through the relative permeability approach, since Levec et al. (1986) showed some success in incorporating multiplicity into this model (see Chapter 2). Figure 16 shows the liquid and gas phase relative permeabilities as functions of the reduced liquid and gas phase saturations. In this figure, the experimental pressure drop values were inserted into equations 7 and 8 to obtain k_L and k_G. These are then plotted against their associated holdups (reduced liquid saturation) for each mode. The functional dependencies of relative permeability on phase saturation compare well with those obtained by Levec et al. (1986) for k_L in the Levec (2.0 vs. 2.0)

and Kan-Liquid (3.5 vs. 2.9) modes. Likewise, for k_G, the powers of β_G for the Kan-Liquid/Super modes also compare well (3.3 vs. 3.6).

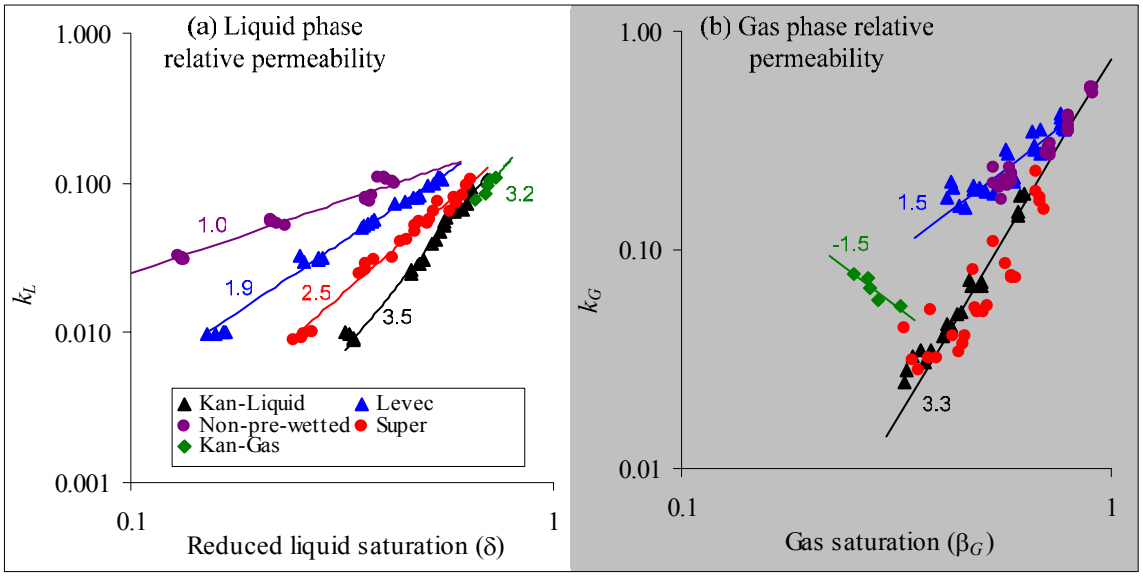

Figure 16. Liquid and gas relative permeabilities as functions of the phase saturations. Numbers on the lines indicate approximate slopes that correspond to the power of the saturation in equations 9 and 10.

The peculiarity of the Kan-Gas mode is apparent in Figure 16b where the negative slope indicates that lower pressure drop is associated with lower gas saturation (i.e. higher holdup). Figure 16 suggests that the relatively simple way used by Levec et al. (1986) to model multiplicity can be extended to incorporate the additional modes as well by writing expressions analogous to equations 9 and 10 for each mode. There are two problems with this. The first is that there are (at least) two equations per mode (one for liquid and one for gas relative permeability) and that each of these has two fitted parameters (the power of the saturation which determines how permeability changes with velocity and the coefficient that determines the basis from which it changes). To model all 5 modes there are 2×2×5 = 20 fitted parameters. In attempting to obtain such a model for the present data, it was found that these 20 parameters were all different and could only be determined empirically. The second problem is that the functional form of the equation (power law), only works well at the lower end of velocities. This cannot be seen from Figure 16 because a log-scale is used, but was illustrated in Figure 10. For these reasons

relative permeability is used here only in a qualitative sense. From Figure 16a it is seen that the slope increases in the order Non-pre-wetted, Levec, Super, Kan-Gas and Kan-Liquid. Now, two other slopes are well known, namely a slope of 3 for a uniformly wetted packed bed (Nemec et al., 2005b) and a slope of 2 for flow in a vertical cylinder (Fourar et al., 2001). Flow in the Levec mode therefore corresponds closely to flow in a cylinder (which is again reminiscent of "rivulet" flow), while flow in the Kan-type modes corresponds to more uniform, fully wetted flow in a packed bed. The slopes of these lines can therefore be seen as a measure of the flow uniformity (but does not in itself describes how the specific flow type is established). This issue is returned to in Chapter 7.

Appropriateness of the Limiting Cases Framework

Another major issue requires experimental validation, namely the appropriateness of the limiting cases framework that was introduced at the start of this work. In Figure 5, gas and liquid flow rate variation induced hysteresis loops were reported for some of the modes. Using the same setup as before, additional gas and liquid flow rate loops were conducted after the bed had been put into each of the five multiplicity modes. The experimental details are given in Van der Westhuizen (2006) and the results are shown qualitatively in Figure 17. The results were generated by establishing steady state at $u_L = 5$ mm/s and $u_G = 2$ cm/s, and then increasing liquid velocity to 7 and 9 mm/s followed by decreasing it back to 7 and 5. The gas loops were conducted by establishing steady state at $u_L = 5$ mm/s and $u_G = 2$ cm/s, and then changing gas flow as follows: 2, 4, 7, 4, 2 cm/s. The data support the idea of using the limiting modes because flow rate variation simply results in moving around *in-between* the 5 modes (no limits crossed). For example, the maximum pressure drop is obtained in the Kan-Liquid mode and conducting gas or liquid flow rate loops does not cross this boundary – the Kan-Liquid mode is therefore the absolute upper limit of pressure drop that can be achieved through manipulation of the hydrodynamic state.

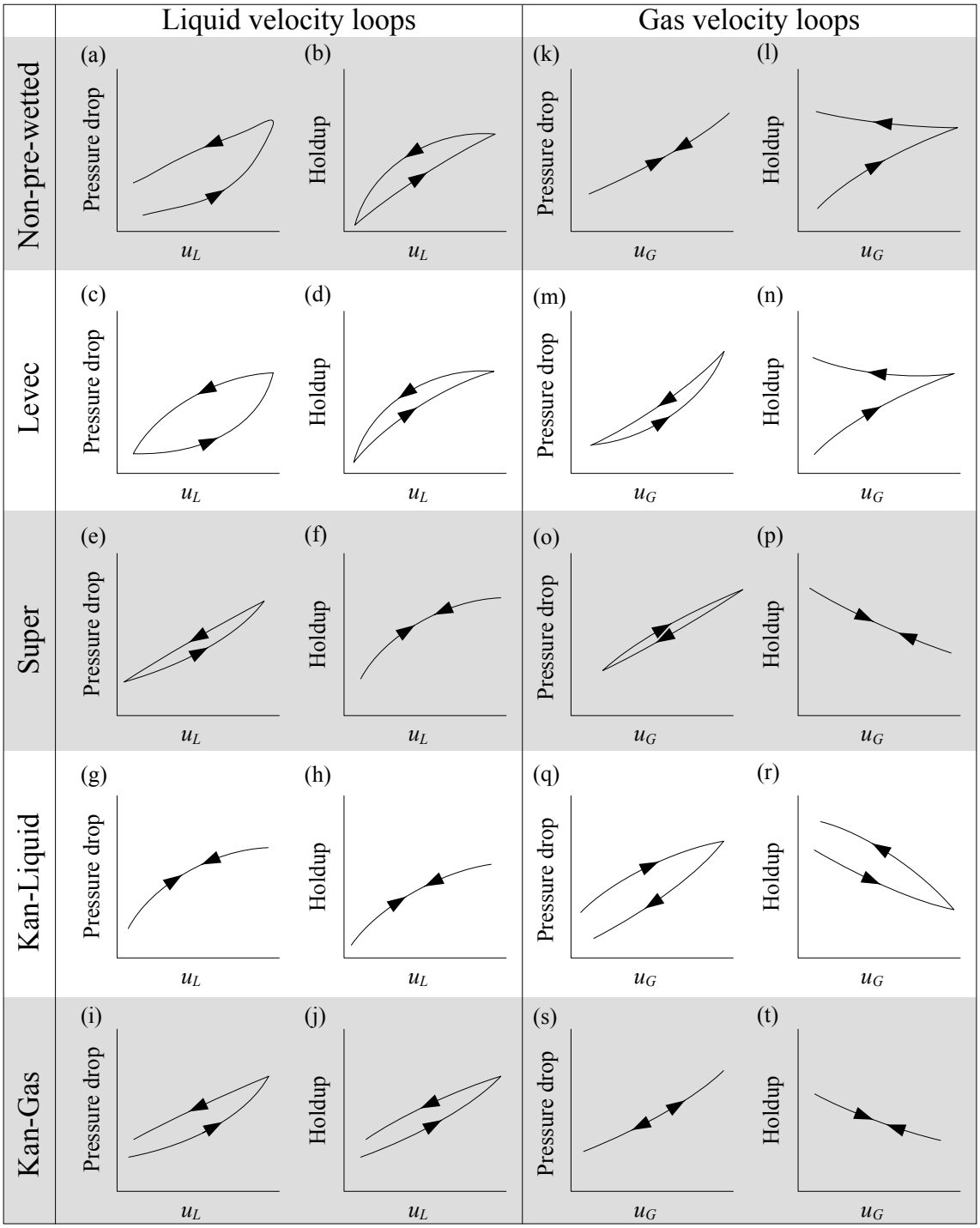

Figure 17. Gas and liquid flow rate induced hysteresis loops in all the hydrodynamic modes (a complete version of Figure 5).

An additional example is the fact that no flow rate manipulation (gas or liquid) can cross the lower boundaries (the minimum cases are still the Non-pre-wetted and Levec (for pre-wetted beds) modes. See Figure 17a to Figure 17d, as well as Figure 17k to Figure 17n.

The robustness of the limiting cases framework can be tested by conducting repeated loops (of gas or liquid) and to see whether there is any drift to the base value of the hydrodynamic parameter. This is akin to the experiments of repeated loops done by Ravindra et al. (1997b) and discussed in detail by Maiti et al. (2005). Some results are shown in Figure 18, where 10 liquid (Figure 18a) and gas (Figure 18b) flow loops were conducted in each mode.

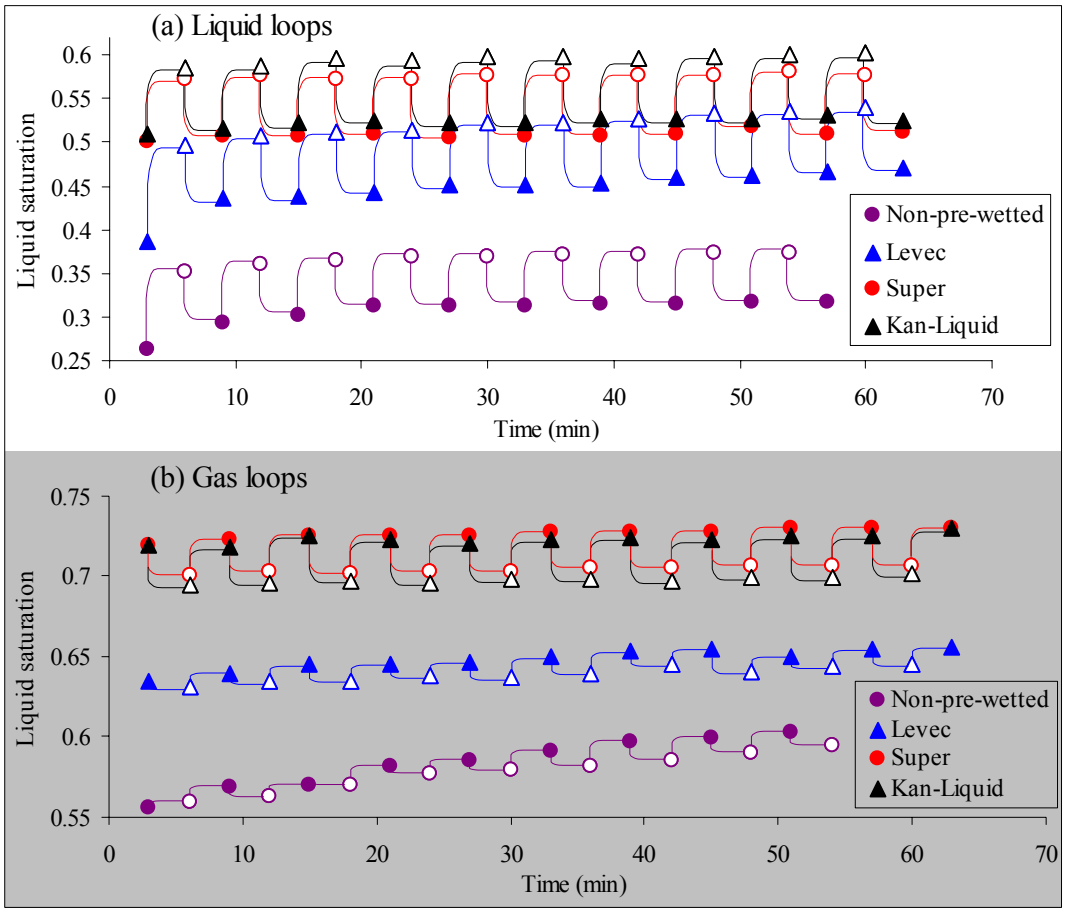

Figure 18. Effect of repeated flow rate variation loops on liquid saturation. In most cases little drift is observed after 2 loops (a) Filled symbols: u_L = 5 mm/s, open symbols: u_L = 7 mm/s. (b) Filled symbols: u_G = 2 cm/s, open symbols: u_G = 4 cm/s.

The liquid loops were performed by establishing steady state in the desired multiplicity mode and then increasing and decreasing the liquid velocity (from 5 to 7 back to 5 mm/s) at one minute intervals, all at a constant gas velocity of 2 cm/s. Similarly, during the gas loops the gas velocity was changed from 2 to 4 and back to 2 cm/s while keeping the liquid velocity at 5 mm/s. The modes are somewhat insensitive to repeated small perturbations of the fluid flow rates. As a specific example, examine the behaviour of the Non-pre-wetted mode at 5 mm/s (Figure 18a): The initial liquid saturation is approximately 0.26. After one liquid loop, the saturation has increased to approximately 0.30 (as expected). On completion of the second loop, it has risen to 0.31 and then stays roughly equal to that upon completion of loops 3 to 10. Importantly, the so-called lower branches (Non-pre-wetted and Levec modes) do not rapidly evolve into the upper ones (Kan-Liquid and Super) over time because of small liquid flow rate changes. The Levec mode also shows no drift with gas flow rate perturbations, although the Non-pre-wetted mode does.

A further aspect of hydrodynamic multiplicity that can be investigated at the bed scale is the impact that a lowering of the surface tension has on the extent of multiplicity. This is presented in two ways in Figure 19. In Figure 19a a liquid flow rate variation induced pressure drop hysteresis loop (starting from the Levec mode) *with a low surface tension liquid* (0.02-0.03 N/m) is compared to the same loop with a high surface tension liquid (0.07 N/m). Gas flow loops show similar behaviour. Experimental details are again reported in Van der Westhuizen (2006) and the present discussion is limited to the evaluation of the data. As noted by several other investigators (Kan & Greenfield, 1978, Levec et al., 1986, Wang et al., 1995), the result is simply that the pressure drop in each mode is now higher, but the hydrodynamic multiplicity is still there. Clear from this figure is the fact that the pulsing boundary is reached at lower liquid velocity for the low surface tension liquid, meaning that the range of liquid velocities where multiplicity is encountered is reduced (from 0-15 mm/s to 0-7 mm/s). Here again is another trend to be included into the list that will be rationalized in terms of the multiplicity mechanism

proposed in Chapter 7. In Figure 19b the effect of a temporary lowering in the surface tension is illustrated. After steady state had been established in the applicable mode, the liquid feed was switched from water to the low surface tension liquid for 3 minutes before it was switched back to water again. Figure 19b shows that the hydrodynamic state of the Kan-Liquid mode is not altered by the temporary reduction in surface tension, while the Levec mode advances toward the upper modes. One way to interpret this is that the temporary reduction in surface tension results in irreversibly increased liquid spreading for the Levec mode but not for the Kan-Liquid mode (since there the liquid is already well spread). This is yet another multiplicity trend that will be re-examined in Chapter 7.

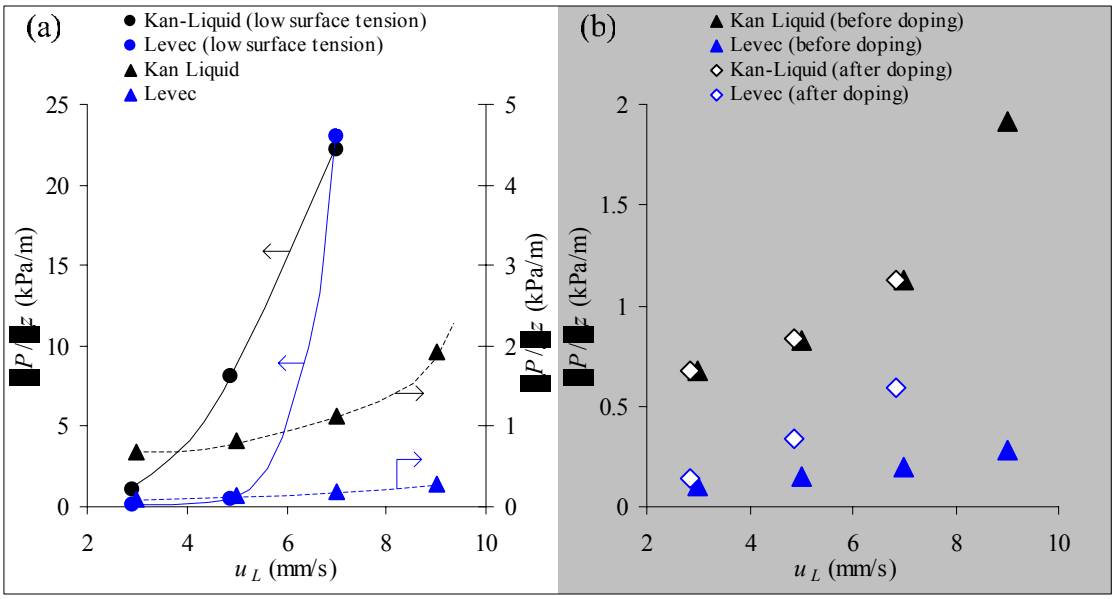

Figure 19. The effect of surface tension changes on hydrodynamic multiplicity. (a) A liquid velocity hysteresis loop with a low surface tension liquid at u_G = 2 cm/s (note that two y-axis scales are used) (b) The effect of surfactant doping, i.e. a surface tension change induced hysteresis loop.

It is concluded from these discussions that the limiting cases framework is both applicable to and useful for the investigation of hydrodynamic multiplicity. The reasons are:

- The 5 modes are distinct and all 5 are important limiting cases.

- *Major* changes in hydrodynamic parameters (at specific conditions) can *only* be brought about by changing from mode to mode.
- Flow rate or surface tension manipulation cannot result in conditions *outside* those of the limiting modes. This is true even for repeated loops.
- It is possible to switch from any mode to any other mode if appropriate procedures are followed.

Figure 20 is presented as a guide to these five modes of hydrodynamic multiplicity and the processes that can be adopted to alter the hydrodynamic state from one mode to any other.

4.3 Multiplicity in Beds of Porous Particles

The wettability of the solid is generally expected to play a big role in determining the hydrodynamics of trickle flow. In the previous section, glass beads were used exclusively in investigating hydrodynamic multiplicity. The equilibrium liquid-solid contact angle at the glass-liquid-solid contact line for glass-air-water is equal to 32 degrees (Van der Merwe et al., 2004). In industrial trickle bed reactors porous particles are predominantly used and the equilibrium contact angle can be expected to be close to zero. Using only the pressure drop hysteresis data of Ravindra et al. (1997b), Maiti et al. (2005) presented a detailed analysis of the differences between hysteresis loops in porous and non-porous beds and paid particular attention to the behaviour of the pressure drop with repeated gas or liquid flow rate cycles. In their work, the idea of "open" and "closed" hysteresis loops is introduced, the former being a hysteresis loop where the pressure drop on the decreasing leg is higher than that of the increasing leg *at the lowest velocity tested*. Since the choice of this lowest velocity is arbitrary (Ravindra et al. chose 1 mm/s) it is unclear exactly what the value of this distinction is. More specifically, *all* hysteresis loops in pre-wetted beds are ultimately closed if this lowest liquid velocity is chosen close enough to zero (at which point the holdup converges to the residual holdup).

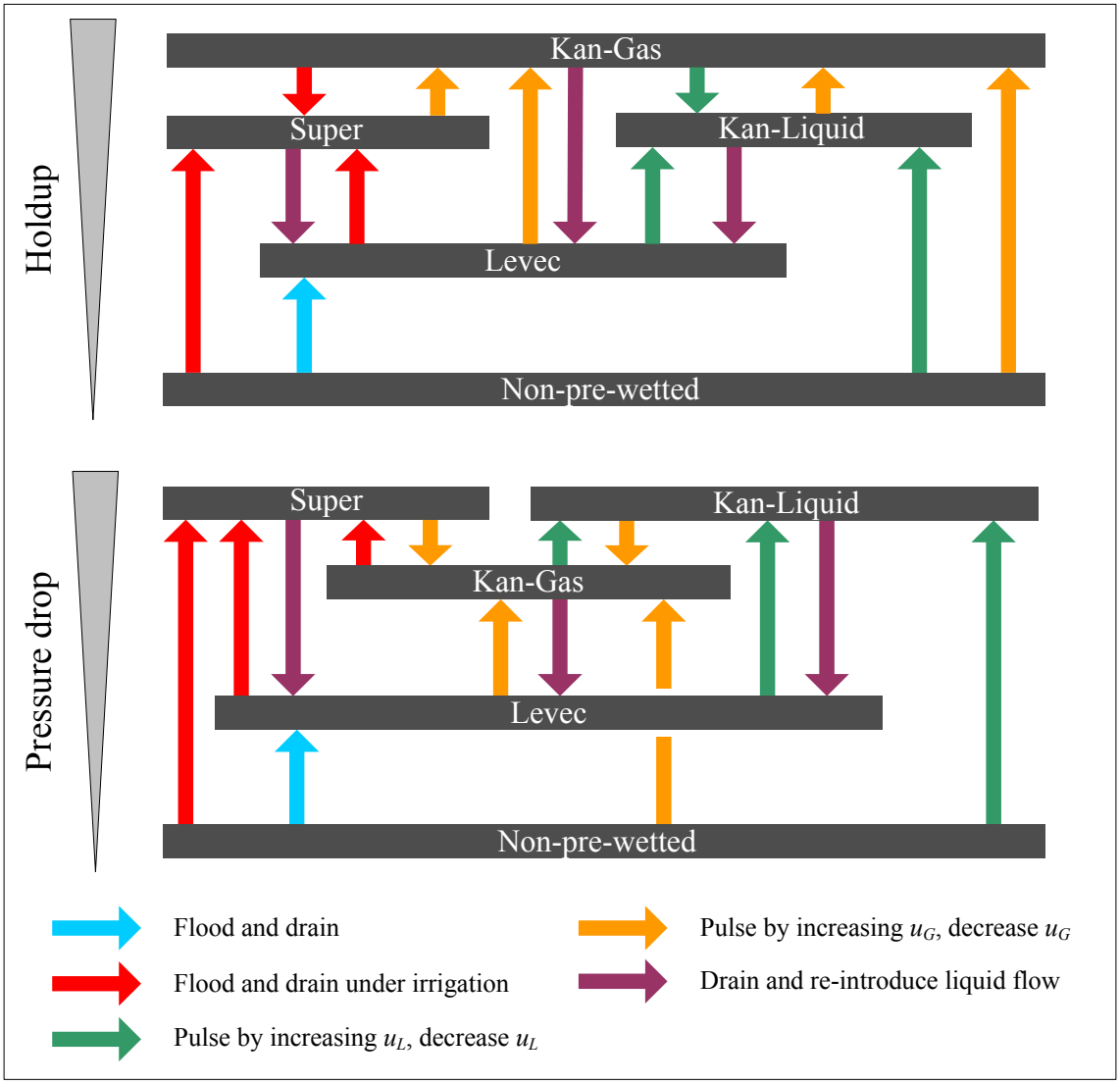

Figure 20. The limiting cases of hydrodynamic multiplicity and their inter-relationships. The limiting cases for gas-liquid mass transfer are the same as those for pressure drop.

However, Maiti et al. (2005) presents two very important ideas:

- The liquid spreading mechanism is different for porous and non-porous particles. In porous particles, there is an additional "pinning force" that keeps liquid films from retracting as severely as they do in non-porous packing. This obviously impacts the receding contact angle.

- Hysteresis is attributable to the different ways that liquid spreads inside the bed. The authors associates “participating and non-participating particles” and “favourable particle clusters” with this idea.

Because porous and non-porous particles show some differences in hydrodynamics, it is necessary to evaluate porous beds through the framework adopted in this work. For this purpose, this section introduces pressure drop, liquid holdup (saturation) and gas-liquid mass transfer multiplicity data generated for a bed packed with 2.5 mm porous alumina spheres for all the conditions examined in the previous (non-porous) section. Figure 21 shows steady state pressure drop, liquid saturation and gas-liquid mass transfer coefficients for the porous bed at a gas velocity of 4 cm/s. The other gas velocities showed comparable trends. For the porous case, the data is the average of two runs and reproducibility was comparable to the non-porous case. The non-porous data is also shown on these figures for comparison. The functional behaviour of all tested parameters remains the same, as well as the limiting cases that have been defined previously. The pressure drop (Figure 21a) in the bed of porous particles is higher than in the non-porous particles (even more than expected from the smaller particle size, 2.5 vs. 3 mm). The extent of pressure drop multiplicity between the Levec and Kan-Liquid/Super modes appear to be similar to the non-porous case. Holdup evidently does not differ as much as a result of hydrodynamic multiplicity in the porous case, although higher holdup is still achieved in the Super/Kan-Liquid mode than in the Levec mode. The gas-liquid mass transfer coefficient extent of multiplicity is also reduced but is still present. To illustrate this, Figure 22 compares the extent of multiplicity for pre-wetted beds (defined as the ratio of the values in the Kan-Liquid and Levec modes, equation 1) in each of the hydrodynamic parameters at u_G = 4 cm/s and u_L = 5 mm/s. Note that the other gas and liquid velocities showed similar behaviour but is not shown here for the sake of brevity.

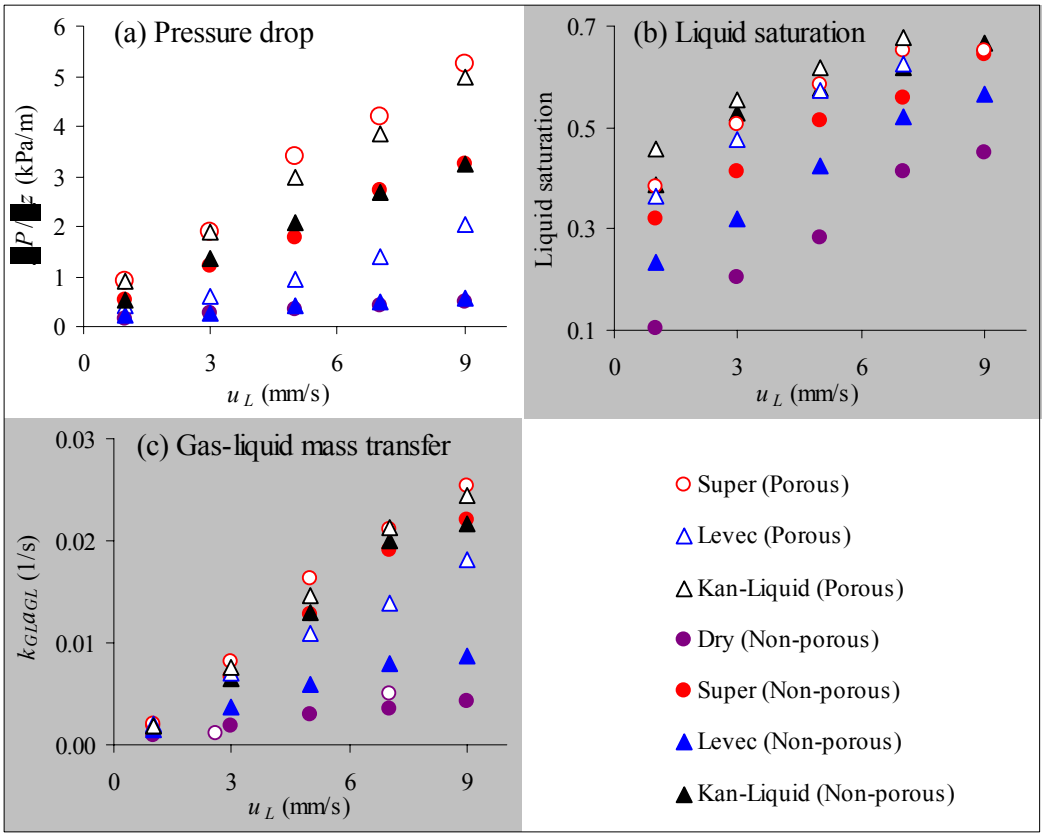

Figure 21. Comparison between porous and non-porous data at $u_G = 4$ cm/s.

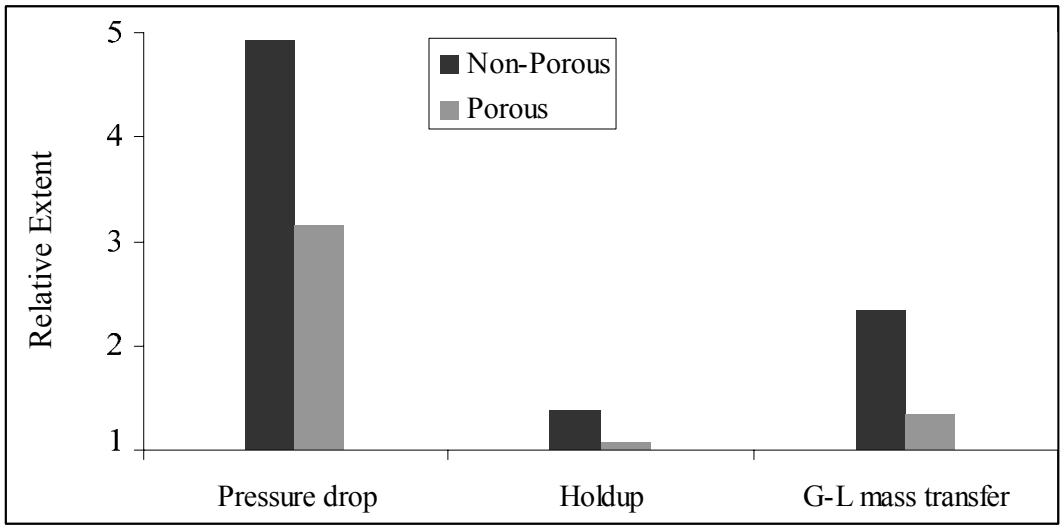

Figure 22. Comparison between the extent of hydrodynamic multiplicity (between the Kan-Liquid and Levec modes) for porous and non-porous packing (at $u_G = 4$ cm/s and $u_L = 5$ mm/s).

Evidently, the porous nature of the packing in the second case serves to aid liquid distribution - but not to the extent of destroying the hydrodynamic multiplicity. The limiting cases framework is valid for porous packing as well. Movement from one mode to another occurs through an irreversible change in the liquid distribution that is caused by either pre-wetting or large liquid or gas flow rate variation. Note that the repeated loop experiments of Ravindra et al. (1997b) is a sub-class of such movement in between modes: the first time a liquid flow rate loop is conducted in a Non-pre-wetted bed, the hydrodynamic state moves upward (see Figure 20) irreversibly and subsequent loops then work off this new base. The same behaviour is seen in Figure 18. Using a porous packing simply changes the extent of hydrodynamic multiplicity, but it is still present and has the same functional behaviour as in beds of non-porous packing.

The effect of particle shape on the hydrodynamic behaviour in the different modes is also of interest because catalyst shapes range from spherical (as used thus far) to cylinders and tri-lobes of very low sphericity. Figure 23 presents some pressure drop multiplicity results for porous alumina cylinders (3×3 mm, sphericity = 0.41) at two gas velocities and different liquid velocities. It is evident that the pressure drops for the extrudate were higher than for the spheres (which corresponds to the trend listed in Chapter 2 - pressure drop is higher when sphericity is lower) and that the pulsing regime is reached at lower liquid velocities for extrudates (the pressure drops in the Levec and Kan-Liquid modes nearly being equal at the top liquid velocity). Apart from these observations, the hydrodynamic multiplicity seems unaffected. The average extent (the average ratio of pressure drop in the two modes for all the liquid velocities at a gas velocity) for a gas velocity of 2 cm/s is 1.9 in both cases, but at u_G = 6 cm/s it is 1.5 for the spheres and 0.7 for the extrudates. This means that hydrodynamic multiplicity is somewhat diminished for the extrudates at high gas velocity compared to the spheres. The rapidity with which the pulsing boundary is reached upon increasing the liquid velocity is clearly associated with the extent of multiplicity (another trend to add to the Trends list). This was also seen in Figure 6 with respect to the effect of gas velocity.

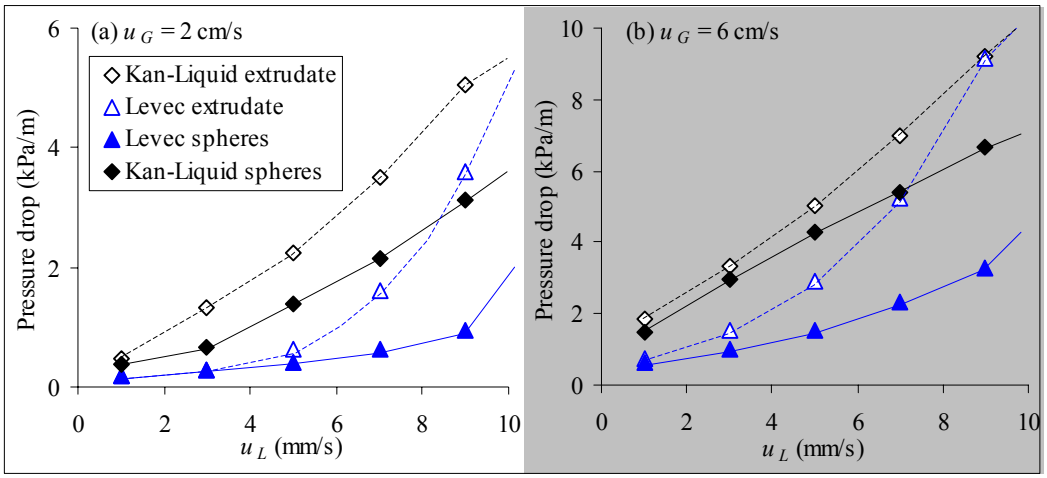

Figure 23. Pressure drop multiplicity as a function of liquid velocity for porous spheres and porous extrudate at two gas velocities.

4.4 The Effect of High Pressure Operation on Hydrodynamic Multiplicity[2]

Insofar as wetting efficiency, holdup and pressure drop in the Kan-Liquid mode is concerned, Al-Dahhan et al. (1995a) showed that an increase in the operational pressure is equivalent to an increase in the density of the gas phase. An important conclusion reached by the same authors is that the increased pressure therefore results in increased gas-liquid drag which in turn causes the liquid to spread more uniformly over the packing surface. This manifests as a simultaneous increase in wetting efficiency and decrease in holdup. Insofar as hydrodynamic multiplicity is concerned, it has been repeatedly mentioned throughout Chapter 2 that the liquid distribution is critically linked to the phenomenon.

If an increased pressure results in increased liquid distribution, it is likely that it will reduce the extent of hydrodynamic multiplicity. For trickle bed reactors specifically, the relevant range of gas densities can be calculated from typical operating conditions. The

[2] The work in this section was conducted at the Chemical Reaction Engineering Laboratory (CREL) at Washington University in St Louis, USA. It is to be published shortly following presentation at the annual AIChE meeting (2007).

conditions range from atmospheric pressure to several MPa. In hydroprocessing (H_2 as gas phase), the pressures range from 1 to 20 MPa at temperatures of 300 to 400 degrees Centigrade (Kundu et al., 2003), putting the gas density approximately in the range 0.4 to 7 kg/m^3. Following Al-Dahhan et al. (1997), these densities can be simulated by air at room temperature at pressures of 30 to 660 kPa (absolute). At low gas density the gas drag effect is negligible (Al-Dahhan et al., 1997). As a consequence, it is the pressures between atmospheric and 0.7 MPa that warrant further investigation. This section presents such data for the experimental conditions listed in Table 13. Additional detail on the construction of the experimental setup is discussed in Lanfrey (2006). Note that the column diameter is larger than what has been previously used. This was an unfortunate experimental constraint that could not be avoided.

Table 13. Experimental details of high pressure experiments

Fluids	Water, Air
Gas pressures	0.1, 0.3, 0.5, 0.7 MPa (absolute)
Gas densities	1.1, 3.3, 5.5, 7.7 kg/m^3
Particles	3 mm non-porous glass spheres
Column diameter	163 mm
Bed length	686 mm
Liquid velocity	1.9, 3.6, 6.7 and 9.5 mm/s
Gas velocity	3.5, 5.7 and 9.2 cm/s
Scale	Resolution: 50 g, maximum load: 220 kg
Differential pressure transducer	Validyne DP15-30 (accuracy: ±20 Pa)
Bed porosity	0.41
Distributor drip point density	11500 points per m^2

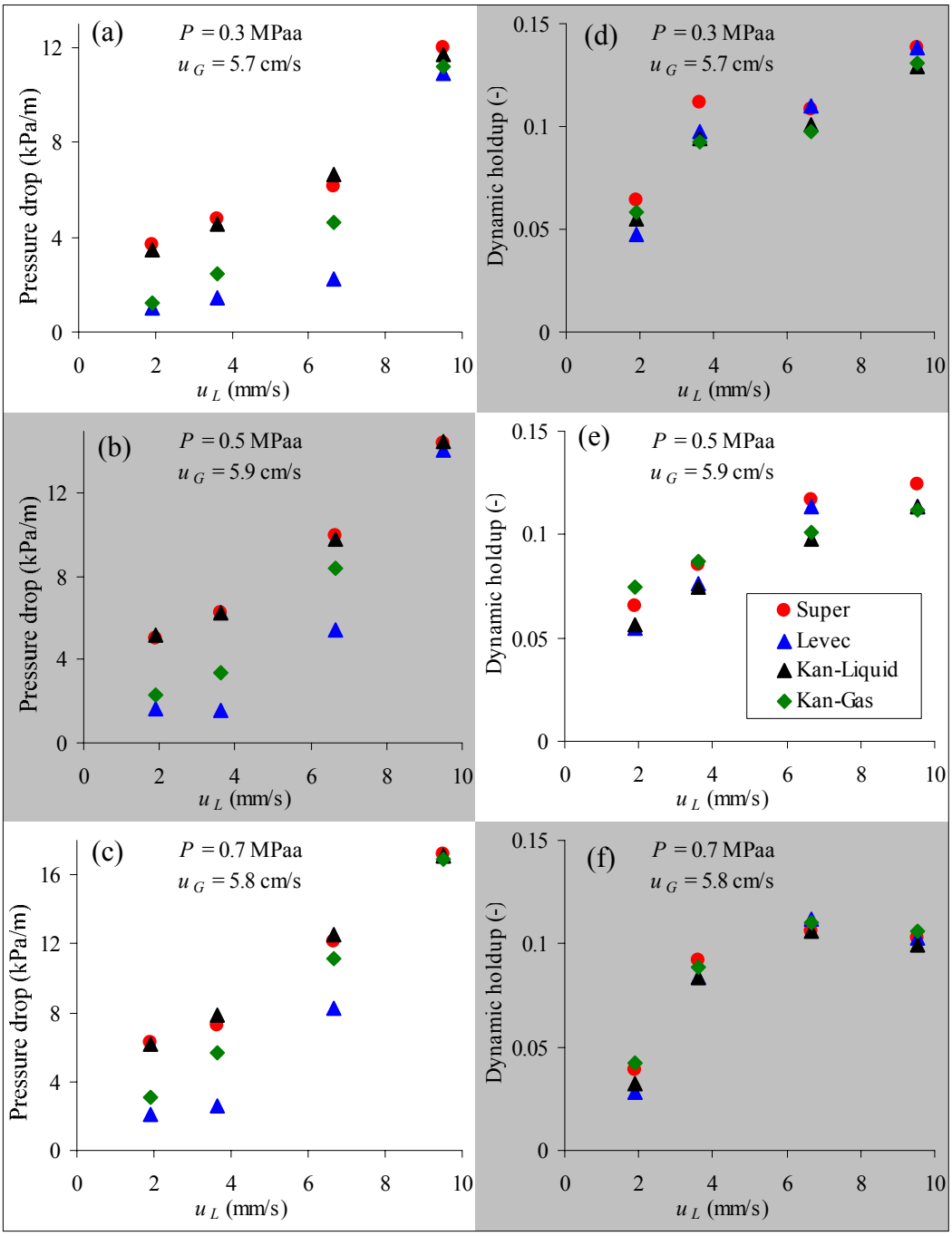

Figure 24. Pressure drop (a-c) and dynamic holdup (d-f) data at increasing pressure ($u_G \approx 5.7$ cm/s)

Results are presented in Figure 24 and Figure 25. The results are shown for u_G = 5.7 cm/s; the other gas velocities showed similar trends. In these figures, each data point is

the average of 2 measurements. Reproducibility was generally within 12-15%, with the pressure drop in the Levec mode being an exception (differences between successive runs were as high as 40%). The Non-pre-wetted mode could not be as extensively studied because of difficulty in loading and unloading the reactor. The results show that the holdup appears to be very similar to one another in the four modes regardless of the pressure. It should be stated that there are severe difficulties in making accurate weight measurements on the scale employed here. Not only is the objective to measure relatively small changes in weight from a large base, the end effects like the weight of the fluid supply lines and the collector installed at the bottom of the column are difficult to compensate for. In each case, a run at equivalent conditions but without the packing was subtracted from the data in an attempt to minimize these effects. The pressure drop measurements do not suffer from these uncertainties and are therefore preferred in subsequent analyses.

From Figure 24a to Figure 24c it is seen that the same trends are followed as the atmospheric pressure case discussed earlier (the limiting cases remain the same). Some additional information is presented in Figure 25, where the pressure drop in each mode is shown for all four pressures as a function of liquid velocity. An increase in pressure results in an increase in pressure drop for all hydrodynamic modes, although this effect is more pronounced in the Levec mode (Figure 25d).

Figure 26 shows the pressure drop ratio of Levec to Kan-Liquid (i.e. 1/Extent) as a function of the gas mass flux for different liquid velocities (Figure 26a) and as a function of the liquid velocity for different gas mass fluxes (Figure 26b). Figure 26a shows the importance of the liquid velocity – increasing the gas mass flux at low velocity has no effect on the extent of multiplicity. Figure 26b clearly shows that an increase in the gas mass flux at medium to high liquid velocity decreases the extent of hydrodynamic multiplicity.

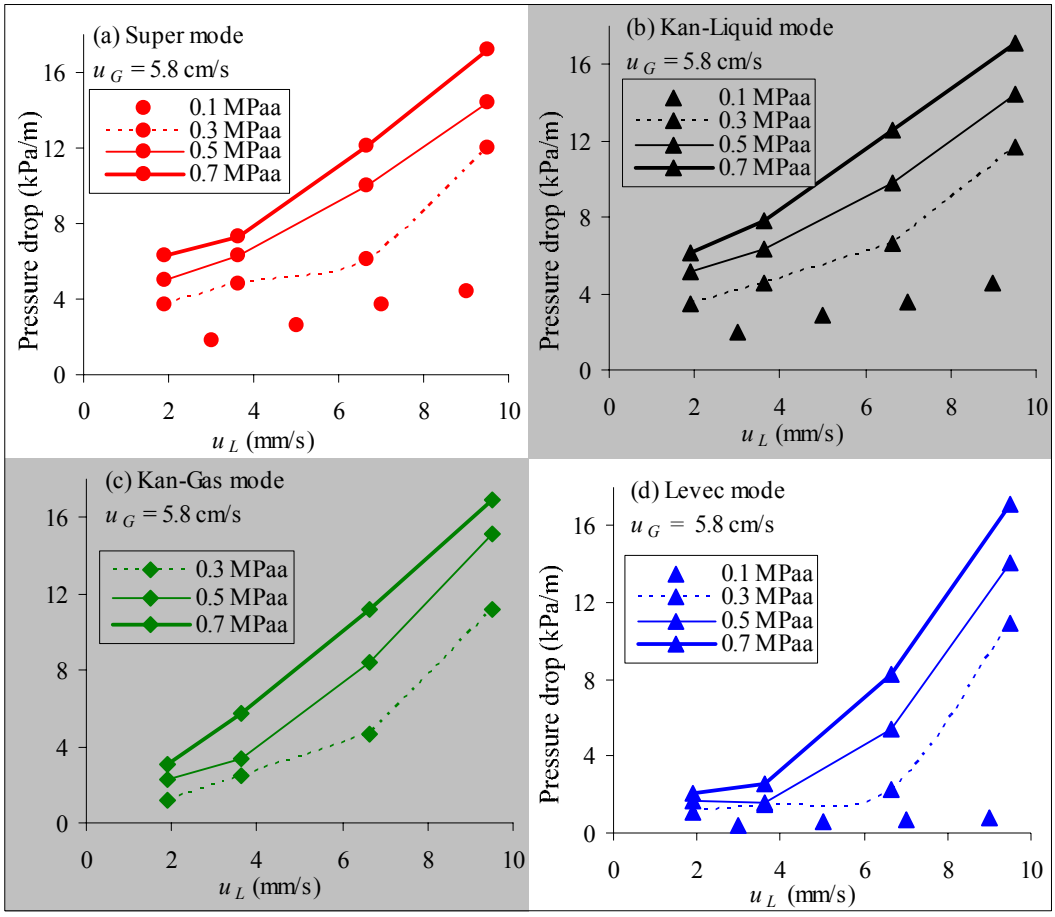

Figure 25. Pressure drop data at increasing pressure per mode (u_G = 5.8 cm/s)

Note that:

- Hydrodynamic multiplicity persists at low liquid velocities even at the highest gas velocity and highest pressure. Increasing either the gas velocity or pressure at low liquid velocity does not decrease the extent of multiplicity.
- At high liquid velocity there is little multiplicity (the pressure drop being equal in both modes).
- At medium to high liquid velocity an increase in gas velocity at constant pressure decreases the extent of multiplicity. Conversely, at medium to high liquid velocity an increase in operating pressure at constant gas velocity also decreases the extent of multiplicity.

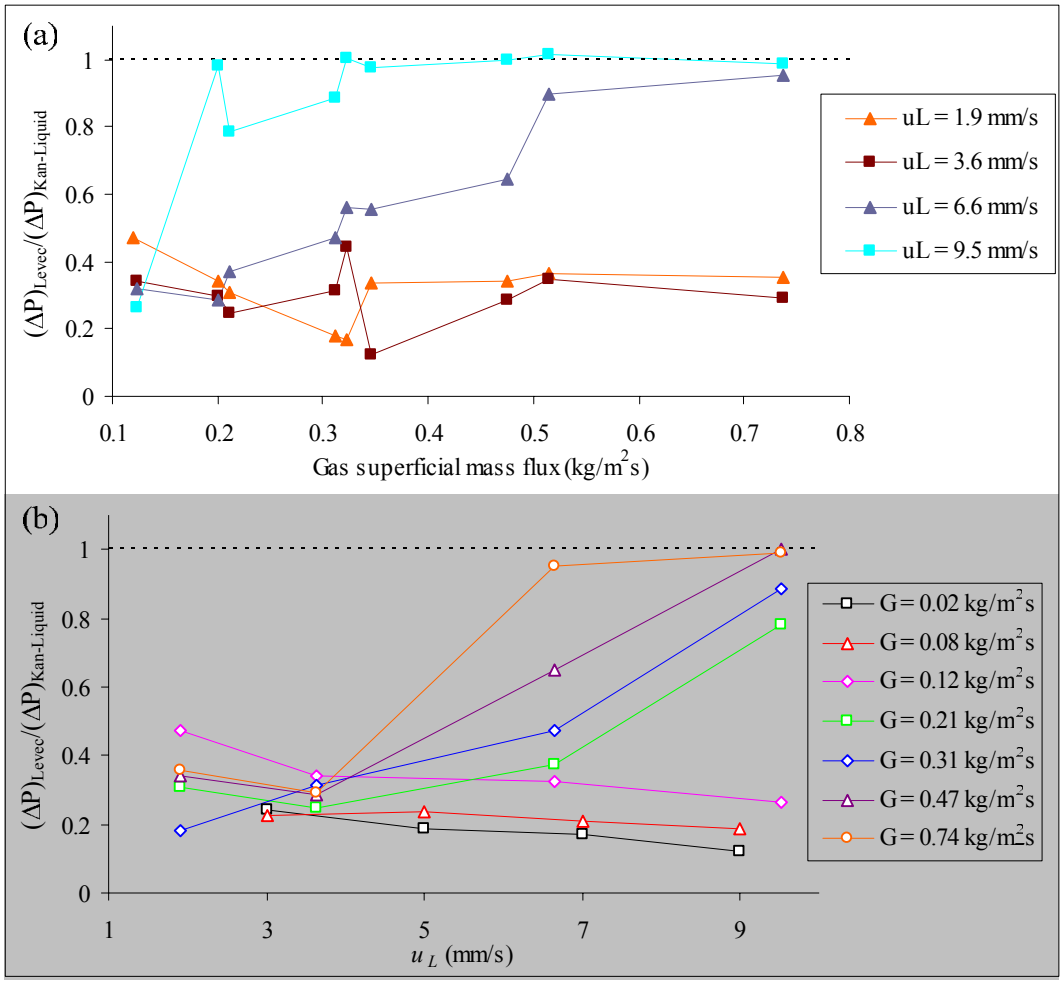

Figure 26. The ratio of Levec to Kan-Liquid pressure drops as a function of (a) gas superficial mass flux liquid and (b) liquid velocity.

The implications of these observations are that the *pressure drop* itself is the governing variable, since whenever pressure drop is high, the multiplicity extent is low and whenever it is low the extent is high. Figure 27 shows the ratio (inverse of extent of multiplicity) against the pressure drop in the Levec mode. Note that all the different conditions fall on one line. This means that for a specific bed, the pressure drop in the Levec mode determines the extent of hydrodynamic multiplicity.

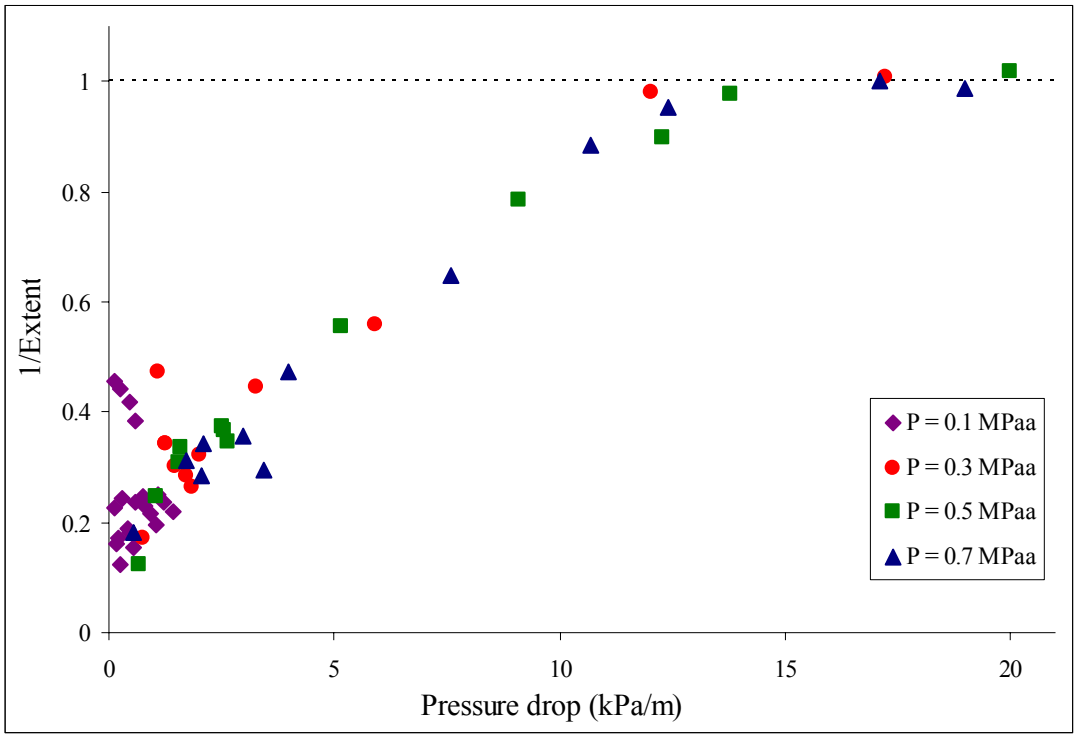

Figure 27. The ratio of Levec to Kan-Liquid pressure drops as a function of pressure drop in the Levec mode. Note that a ratio of 1 (black dashed line) implies that there is no difference in the pressure drop and therefore no hydrodynamic multiplicity.

It is concluded therefore that an increase in operating pressure for the range of industrially important pressures (gas densities) decreases the extent of hydrodynamic multiplicity provided that the liquid velocity is high. At low velocities, the operating pressure has little effect on the extent of multiplicity. High pressure operation therefore causes two major effects: *pressure drop is comparatively much higher (especially in the Levec mode) and multiplicity is less severe at high pressure drop*.

4.5 Conclusions

In this chapter, hydrodynamic multiplicity was investigated at the bed scale through pressure drop, liquid holdup and volumetric gas-liquid mass transfer measurements at conditions that included low and high pressures, porous and non-porous packing elements

and high and low surface tension liquids. This chapter also evaluated the proposed limiting cases of hydrodynamic multiplicity (the conceptual framework) and found them to be a handy framework by which to study pre-wetting and hysteresis in trickle flow. The existing bed-scale literature data are encompassed within this framework.

In accordance with the strategy in Figure 1, a number of trends were identified from new hydrodynamic data in terms of the behaviour of the various hydrodynamic parameters in each limiting mode, as well as how the modes are related to each other. In addition, some of the trends already identified in Chapter 2 were confirmed: **(A)** to **(D)**. The updated list of multiplicity trends is:

(A) There are different flow patterns in the different modes: rivulet-type flow in the lower limiting cases and film-type flow in the upper limiting cases. New rivulets are created as u_L increases.

(B) Liquid flow rate variation induced hysteresis causes increases in pressure drop and liquid holdup in the non-pre-wetted and Levec modes.

(C) Gas flow rate variation induced hysteresis causes increases in pressure drop and holdup in the Levec mode, but an increase in holdup and a decrease in pressure drop in the Kan-Liquid mode.

(D) The extent of pressure drop hysteresis is diminished when particle size is increased.

(E) The Levec mode *wetting efficiency* is lower on average and shows a bi-modal particle wetting distribution, whereas the Super mode shows a Gaussian distribution.

(F) The liquid *holdup* increases by mode in the order Non-pre-wetted, Levec, Kan-Liquid/Super and then the Kan-Gas mode.

(G) The *pressure drop* for the Non-pre-wetted and Levec modes are the same and lower than the Kan-Liquid/Super mode pressure drop. The Kan-Gas pressure drop is in between these despite it having a *larger* holdup.

(H) The *volumetric gas-liquid mass transfer coefficient* shows the same functional behaviour as the pressure drop.

(I) The *Super and Kan-Liquid modes have similar behaviour*, both in the uniformity of the flow distribution and in the nearly identical values in all the hydrodynamic parameters - despite having been established with different operating procedures.

(J) *Small flow rate changes* have little effect on the hydrodynamic multiplicity after the first or second cycle.

(K) A *decrease in surface tension* brings the pulsing boundary to lower liquid velocity, but hydrodynamic multiplicity still persists in the trickle regime.

(L) A temporary decrease in the surface tension (*surface tension change induced hysteresis*) has no effect on the pressure drop in the Kan-Liquid mode but increases the pressure drop in the Levec mode.

(M) Beds of porous particles have a lower extent of multiplicity compared to beds of non-porous particles.

(N) The extent of multiplicity is associated with the pulsing boundary; *hysteresis is diminished if the pulsing boundary velocity is lowered* (by changing surface tension or particle shape).

(O) An increase in liquid or gas velocity in the *Levec mode drastically increases the pressure drop* at high pressure (gas density), while the increase in the other modes is far less drastic.

(P) High pressure operation (or high gas mass flux) has little effect on multiplicity at low liquid velocity, but decreases the extent of multiplicity at high liquid velocity. The *pressure drop determines the extent of multiplicity*.

Note that these trends all refer to bed-scale averages of the hydrodynamic parameters. However, as discussed in section 2.3.2, several authors have suggested that the bed-scale observations are the results of phenomena that occur at the micro-scale (pore-scale). Therefore, there is reason to expect the governing mechanism for hydrodynamic

multiplicity to be easier identifiable at the pore-scale. This requires pore-scale hydrodynamic data, which is obtained through radio-imaging in the next two chapters.